Published in final edited form as:
Langmuir. 2009 July 7; 25(13): 7279–7286. doi:10.1021/la900310k.

Effect of the lipid chain melting transition on the stability of DSPE-PEG(2000) micelles

Mark Kastantin[1], **Badriprasad Ananthanarayanan**[1], **Priya Karmali**[2,3], **Erkki Ruoslahti**[2,3,4], and **Matthew Tirrell**[1,5]

[1]Department of Chemical Engineering, University of California, Santa Barbara, California 93106

[2]Vascular Mapping Center, Burnham Institute for Medical Research at UCSB

[3]Cancer Research Center, Burnham Institute for Medical Research, La Jolla, California, 92037

[4]Department of Molecular, Cellular, and Developmental Biology, UCSB

[5]Materials Research Laboratory, UCSB

Abstract

Micellar nanoparticles are showing promise as carriers of diagnostic and therapeutic biofunctionality, leading to increased interest in their properties and behavior, particularly their size, shape, and stability. This work investigates the physical chemistry of micelles formed from DSPE-PEG(2000) monomers as it pertains to these properties. A melting transition in the lipid core of spheroidal DSPE-PEG(2000) micelles is observed as an endothermic peak at 12.8°C upon heating in differential scanning calorimetry thermograms. Bulky PEG(2000) head groups prevent regular crystalline packing of lipids in both the low-temperature glassy and high-temperature fluid phases, as evidenced by wide-angle x-ray scattering. Equilibrium micelle geometry is spheroidal above and below the transition temperature indicating that the entropic penalty to force the PEG brush into flat geometry is greater than the enthalpic benefit to the glassy core to pack in an extended configuration. Increased micelle stability is seen in the glassy phase with monomer desorption rates significantly lower than in the fluid phase. Activation energies for monomer desorption are 156 ± 6.7 and 79 ± 5.0 kJ/mol for the glassy and fluid phases, respectively. The observation of a glass transition that increases micelle stability but does not perturb micelle geometry is useful for the design of more effective biofunctional micelles.

Introduction

Micelles formed from 1,2-distearoyl-sn-glycero-3-phosphoethanolamine-N-[methoxy (polyethylene glycol)-2000] (DSPE-PEG(2000), or generally PEG-lipid) have shown promise as nanoparticles for drug delivery.[1–3] DSPE-PEG(2000) and similar PEG-lipid monomers have been used to create micelles capable of solubilizing hydrophobic drugs or incorporating imaging agents, and delivering them to specific locations via targeting ligands conjugated to a fraction of the monomer units.[4–8] Biological functionality of the micelles can be in the form of hydrophobic cargo sequestered in the micelle core as well as hydrophilic targeting or imaging agents conjugated to the free end of the PEG chains in the corona.

In aqueous solution, DSPE-PEG(2000) micelles are oblate spheroids with a maximum diameter of 18 nm and an aggregation number near 90.[9] Small size alone gives these micelles favorable properties for *in vivo* drug delivery since extravasation, tissue localization and cellular uptake

Correspondence to: Matthew Tirrell.

are facilitated by small particle size. Smaller particles accumulate in pathological tissues with leaky vasculature via the enhanced permeability and retention effect.[10] In addition, small size causes enhanced accumulation in target organs by minimizing nonspecific clearance in reticuloendothelial system tissues like the liver and spleen.[11] Furthermore, the mechanism of cellular uptake and subsequent intracellular routing is also affected by size, with smaller particles being internalized via clathrin-coated pits and more likely to reach lysosomes.[12] As a result, small particles reach cellular targets more efficiently, but require a mechanism to escape lysosomal degredation. While there are benefits to the use of small nanoparticles, there is also a need to give them complex function so they can overcome obstacles presented by their small size.

PEG-lipid monomers provide a platform for facile creation of multifunctional micelles that display complex biological signals. This is primarily because PEG-lipid monomers can be created with different chemical functionalities at the free end of the PEG chain that can be used to covalently link peptides or other ligands to the PEG-lipid. Commercially available functional groups for a DSPE-PEG(2000) monomer include: primary amine, carboxylic acid, maleimide, PDP (3-(2-pyridyldithio)propionate) and biotin. These functional groups allow the use of several conjugation strategies to link biological ligands to the PEG-lipid monomer. Consequently, mixing of different monomers leads to multifunctional mixed micelles with precise control over number and ratio of functionalities without the need for orthogonal chemical reactions.

DSPE-PEG(2000) micelles exhibit a low critical micelle concentration (CMC) of approximately 1×10^{-6} M due to the strong hydrophobic driving force for self-assembly originating from two saturated, 18-carbon acyl chains.[13,14] This property is attractive for *in vivo* nanoparticles as the residence time of a monomer in a micelle is inversely proportional to the CMC.[15] This is a consequence of having a highly hydrophobic core to provide a large activation barrier to monomer desorption from the micelle, often the rate-limiting step in micelle breakup.[16,17] For *in vivo* applications, monomers in unstable micelles are more likely to leave the micelle and nonspecifically bind to proteins, thus diminishing any multivalent benefit of a nanoparticle with high ligand density. In the case of mixed micelles, increased stability also means that micelle complexity due to heterogeneity will be retained over a longer period of time. Consequently, stable mixed micelles that are suddenly diluted into blood can retain their original composition for the time required to target and deliver cargo, but will disassemble on longer timescales for clearance from the body. Mixed micelles have indeed shown adequate stability for *in vivo* tumor targeting.[4] However, applications that require long-term targeted therapy would benefit from micelles with greater stability. One such application currently under investigation is targeted delivery of anticoagulant peptides to plaques prone to form thrombi.[8]

This work provides insight into the physical chemistry of the DSPE core as it pertains to micellar stability. Fully hydrated DSPE lipids form lamellar gels at room temperature and have a melting temperature of 74°C.[18] However, DSPE-PEG(2000) micelles have a fluid core at room temperature, as reported by Kenworthy and colleagues.[19] The authors note that PEG-lipid micelles do not undergo endothermic lipid chain melting transitions upon heating, but only examine temperatures above 30°C. The present study identifies such a transition at 12°C that is ascribed to the chain melting transition of lipids in the micelle core. While the transition does not change micelle size and shape, stability of the micelle is higher in the low-temperature condensed phase due a higher activation barrier to monomer desorption from the micelle.

Experimental

Materials

1,2-distearoyl-sn-glycero-3-phosphoethanolamine, 1,2-distearoyl-sn-glycero-3-phosphoethanolamine-N-[methoxy(polyethylene glycol)-1000], 1,2-distearoyl-sn-glycero-3-phosphoethanolamine-N-[methoxy(polyethylene glycol)-2000], 1,2-distearoyl-sn-glycero-3-phosphoethanolamine-N-[maleimide(polyethylene glycol)-2000], and 1,2-dipalmitoyl-sn-glycero-3-phosphoethanolamine-N-[methoxy(polyethylene glycol)-2000] (DSPE, DSPE-PEG(1000), DSPE-PEG(2000), DSPE-PEG(2000)-maleimide, and DPPE-PEG(2000), respectively) were purchased from Avanti Polar Lipids and used without further purification. N-2-hydroxyethylpiperazine-N′-2-ethanesulfonic acid (HEPES) was purchased from Sigma-Aldrich. The resin and all reagents for peptide synthesis were purchased from EMD Biosciences. Dr. Craig Hawker donated polyethylene glycol with average molecular weight 3400 (Sigma-Aldrich) for this work.

Synthesis of peptide-conjugated DSPE-PEG(2000) lipids

A fluorescent peptide sequence was used to label DSPE-PEG(2000) monomers and to demonstrate the effect of the physical state of the micellar core on the stability of peptide-displaying micelles. The chosen sequence, CGSGSGRGAFSG-NH_2 (referred to as RGA), is under investigation as a negative control for cell-adhesion experiments involving the integrin-binding sequence, RGD. The sequence was manually synthesized using standard fluorenylmethoxycarbonyl (Fmoc) chemistry.[20,21] The N-terminus of the peptide was modified by the addition of aminohexanoic acid and subsequently by 5(6)-carboxytetramethylrhodamine to give a fluorescent peptide. After cleavage from the resin, the crude product was purified by reverse-phase high-performance liquid-chromatography (HPLC) using 0.1% TFA in acetonitrile-water mixtures on a C8 preparatory column at 40°C. The fluorescent peptide was 90% – 95% pure by HPLC and was characterized by electrospray ionization time-of-flight mass spectrometry. Fluorescent RGA peptide was conjugated to DSPE-PEG(2000)-maleimide via a thioether linkage to the side-chain thiol on the N-terminal cysteine. A 10% molar excess of the fluorescent peptide was added to the PEG-lipid dissolved in 10% v/v methanol in water. Unreacted peptide was then separated from the DSPE-PEG (2000)-RGA by reverse-phase HPLC on a C4 preparatory column at 60°C using the same solvents as above.

Sample preparation

Lipid and PEG-lipid aggregates were prepared in a glass culture tube by dissolving the monomers in chloroform and evaporating the solution under nitrogen. The resulting film was dried under vacuum for 8 hours and rehydrated in 0.01 M HEPES buffer at 90°C (pH = 7.4, 0.01 M NaCl). PEG-lipid samples were incubated at 90°C for 60 minutes and transferred to a sonicating bath at 70°C for 60 minutes. Samples were subsequently extruded through a 100 nm membrane at 90°C and allowed to cool to room temperature for 6 hours. DSPE films were hydrated at 90°C for 60 minutes, and tip sonicated at room temperature for 2 minutes to form unilamellar vesicles. Sample concentrations were typically 1 wt% for dynamic light scattering (DLS). For differential scanning calorimetry (DSC) or wide-angle x-ray scattering (WAXS), each sample was concentrated after self-assembly, using a centrifugal filter with a nominal molecular weight cutoff of 5000 Da (Millipore). Final concentrations ranged from 4–10 wt%, which were low enough to ensure complete hydration of lipid head groups. One sample of DSPE was also prepared for DSC with PEG(3400) added to the solution in a mass fraction equivalent to that of PEG in DSPE-PEG(2000) samples. In both WAXS and DLS experiments, samples were cooled or heated from room temperature to the measurement temperature at an approximate rate of 0.2°C /minute.

Differential scanning calorimetry

DSC thermograms were obtained on a DSC Q2000 calorimeter (TA Instruments). 75 μl of the sample was filled in a stainless steel pan that was then hermetically sealed to prevent sample evaporation. An empty pan was used as a reference. This results in a baseline that has a slight positive slope; further, a peak due to freezing of water can be detected but this was not observed until subcooling to −20°C and is hence not shown. Scan rates ranging from 5°C /minute to 1° C /minute were used and several heat/cool cycles were performed to ensure that the data represented equilibrium measurements. Presented data are from the steady-state heating cycle at 1°C /minute. Transition temperatures specified in the text correspond to the average of the peak temperatures obtained from the heating and cooling cycles, unless mentioned otherwise. Enthalpy values were obtained by integrating the area under the peak using TA Instruments Universal Analysis 2000 software.

Wide-angle x-ray scattering

WAXS was performed on a custom-built x-ray spectrometer with a large 4-circle goniometer (Huber), a double focusing multiplayer monochromator (Osmic) and a MAR 345 mm diameter image plate detector (Mar Research). The x-ray source was an 18 kW rotating anode x-ray generator (Rigaku) with a copper anode that produced incident radiation with a wavelength of 1.54 Å. Temperature control was provided to within 0.1°C by a circulating water bath and a custom-built sample holder. The system was calibrated using a silver behenate standard. After image collection, detector intensity was circularly averaged to determine scattering intensity as a function of scattering wave vector, q, in the range from q = 1.0 to 2.4 $Å^{-1}$. In this range, scattering intensity is sensitive to intermolecular spacing of strongly scattering atoms. Scattering from oxygen-oxygen pairs in water and carbon-carbon pairs in the micelle core are the primary features observed.

Micelle size as determined by dynamic light scattering

DLS was used to measure particle size as a function of temperature. Temperature was controlled to within 0.1°C using a circulating water bath. The DLS system (Brookhaven Instruments) consisted of an avalanche photodiode detector to measure scattering intensity from a 632.8 nm HeNe laser (Melles Griot) as a function of delay time. The first cumulant of the first-order autocorrelation function (Γ) was measured at a fixed angle of 90° (q = 0.0187 nm^{-1}) and the quantity Γ/q^2 was taken as the apparent diffusion coefficient D_o of the aggregate. The Stokes-Einstein relationship (equation (1)) was then used to estimate a particle size. In equation (1), η is the solvent viscosity, D_o is the diffusion coefficient of the particle, and d_H is the hydrodynamic diameter. It should be noted that although D_o is typically obtained from an extrapolation of Γ/q^2 to q = 0, spherical particles exhibit no q-dependence of this quantity and spheroidal particles with axis ratios near 1 only show weak q-dependence. The simplification due to measuring D_o at a 90° scattering angle produces a slight underestimate of the true hydrodynamic diameter of the particle (typically 2–3 nm for these micelles), but this a constant error as a function of temperature.

$$d_H = \frac{k_B T}{3\pi\eta D_o} \tag{1}$$

Measurement of monomer desorption rates using rhodamine self-quenching

To assess micelle stability, monomer desorption rates from fluorescent micelles were measured as a function of temperature. Self-quenching behavior of rhodamine on the RGA peptide was used to determine the rate at which monomers leave DSPE-PEG(2000)-RGA micelles. In a homogeneous population of DSPE-PEG(2000)-RGA micelles, close physical proximity causes

fluorophores on the micelle to self-quench while free monomers in solution have high fluorescence. At equilibrium, the flux of monomers leaving the micellar state equals the flux leaving the monomeric state and fluorescence intensity remains constant. Upon introduction of a large population of non-fluorescent DSPE-PEG(2000) micelles, DSPE-PEG(2000)-RGA monomers move from quenched micelles to unlabeled micelles and become unquenched, thereby leading to an increase in fluorescence intensity as illustrated in Figure 1. The rate-limiting step in this process is believed to be desorption of the DSPE-PEG(2000)-RGA monomer from the micelle, rather than diffusion to a nearby micelle or incorporation into that micelle.[16,17] The experimentally observed increase in fluorescence intensity therefore provides a measurement of the rate of monomer desorption from the micelle.

In an analogous approach to that of Wimley and Thompson, fluorescence intensity can be modeled as a function of time by equation (2) in which k is the desorption rate constant.[17]

$$I(t)=[I(0)-I(\infty)]e^{-kt}+I(\infty) \quad (2)$$

In developing this equation, it is assumed that the rate-limiting step in monomer exchange is desorption of monomers from the micelle, that exchange occurs between two constant populations of donor and acceptor micelles, that DSPE-PEG(2000)-RGA monomers have equal fluorescence if they incorporate into an unlabeled micelle or remain free in solution, that all monomers are available to leave the micelle, and that the unlabeled, acceptor population of micelles is much greater than the labeled, donor micelles. This last assumption removes the dependence of fluorescence intensity on the relative donor and acceptor concentrations in addition to ensuring that acceptor micelles do not become sufficiently populated with fluorophores that they become quenched.

This analysis neglects the increase in fluorescence caused by replacing one fluorescent monomer with a non-fluorescent monomer in the highly quenched micelle. These effects are not expected to be significant until large values of kt, when the micelle is so sparsely populated with fluorophores that the probability of a fluorophore participating in a quenching event becomes dependent on the number of remaining fluorophores. This effect would cause the appearance of a second rate constant and the measured desorption rate would be faster than the actual rate. In fact, a single apparent rate is observed as given in equation (2), reinforcing that errors from this assumption are minimal.

DSPE-PEG(2000)-RGA micelles were created at a monomer concentration of 2.3×10^{-5} M (0.095 mg/ml) while DSPE-PEG(2000) micelles were created at a monomer concentration of 5.0×10^{-3} M (14 mg/ml). Both micellar solutions were incubated in a temperature-controlled fluorimeter (Cary Eclipse) for 60 minutes. DSPE-PEG(2000) micelles were added to DSPE-PEG(2000)-RGA micelles and the solution agitated with a pipette to promote mixing. After mixing, the concentration of DSPE-PEG(2000) was 7.1×10^{-4} M while that of DPSE-PEG (2000)-RGA was 2.0×10^{-5} M to give an acceptor: donor ratio of 36: 1. Immediately after mixing, fluorescence intensity was recorded at 590 nm (550 nm excitation) as a function of time. Collection times ranged from 90 minutes at 30°C to 1000 minutes at 4°C. Fluorescence was measured 10 times per minute for the first 60 minutes, and once per minute thereafter to minimize photobleaching.

Results

Figure 2 shows heat flow as a function of temperature for the heating of fully hydrated DSPE, DPPE-PEG(2000), DSPE-PEG(1000) and DSPE-PEG(2000) self-assembled structures as measured by DSC. A reversible, first-order phase transition is seen in vesicles composed of

DSPE at its main melting temperature of 74°C. This melting transition is not strongly affected by the mere presence of PEG, as a similar, but slightly broader, transition is still seen at 74°C upon the addition of PEG(3400) to the solution. DSPE-PEG(2000) micelles do not show a melting transition near 74°C. An endothermic peak is seen in this sample at 12.8°C upon heating, which is reversible on cooling at 11.1°C (data not shown). The enthalpy of this reversible phase transition is measured to be 39 ± 4.2 kJ/mol. Several transitions are seen in DSPE-PEG(1000) micelles, the largest of which occurs at 58.0°C upon heating (49.1°C upon cooling); the corresponding transition enthalpy is 35 ± 7.5 kJ/mol. No transition was observed in DPPE-PEG(2000) micelles over the temperature range studied.

WAXS curves are shown in Figure 3 for DSPE, DSPE-PEG(1000) and DSPE-PEG(2000) at 25°C as well as for DSPE-PEG(2000) at 2°C. Scattering from oxygen-oxygen pairs in water is prominent near $q = 2.0$ Å^{-1} in the DSPE sample.[22] A shift in this peak to lower q is often observed in samples containing PEG(2000). This could be due either to a contribution from the PEG backbone itself or the disruption in the hydrogen-bonded structure of water in the presence of PEG(2000). A sharp peak exists near $q = 1.5$ Å^{-1} in the DSPE and DSPE-PEG (1000) samples that is absent in DSPE-PEG(2000) samples both at 2°C and 25°C. This peak is due to scattering from carbon-carbon pairs of the lipid chains packed in a crystalline lattice in gel-phase DSPE lamellae.[23] Scattering from lipids in the core of DSPE-PEG(2000) micelles appears as a broad shoulder on the side of the water peak, near $q = 1.5$ Å^{-1}. Thus, at 25°C, DSPE and DSPE-PEG(1000) exhibit regular packing of lipid chains while DSPE-PEG(2000) remains disordered on both sides of the phase transition seen in Figure 2.

A steady decrease in the hydrodynamic diameter of DSPE-PEG(2000) micelles is seen upon cooling in Figure 4. The range of hydrodynamic diameter observed (10.7–16.0 nm) is consistent with small, spheroidal micelles in both the glassy and fluid phases. Storage of micelles at 5°C for up to 60 days did not result in any change in hydrodynamic diameter, the shape of the autocorrelation function, or its weak q-dependence (data not shown).

The inverse of monomer desorption rate constant, k^{-1}, is plotted as a function of temperature in Figure 5(a). Values of k are determined by fitting equation (2) to the time-dependent fluorescence data (inset). Micelles mix with a time constant of over 30 hours near 5°C but this time constant is less than 1 hour above 20°C.

Monomer desorption from micelles is an activated process in which the high-energy transition state is created when the majority of the hydrophobic lipid tail is solvent-exposed, anchored to the micelle by only a small portion of its length.[16,17] After removal from the micelle core, the monomer gains translational and rotational degrees of freedom to lower its overall energy relative to the high-energy state. Consequently, the temperature-dependence of monomer desorption rates can be described by the Arrhenius equation. Figure 5(b) shows an Arrhenius plot in which the natural logarithm of the monomer desorption rate constant is plotted as a function of inverse absolute temperature. In such a plot, the slope of a best-fit line to the data is proportional to activation energy required to reach the transition state from the ground state. In Figure 5(b), data points above 15°C appear to fall on a separate line than those below, further indicating the presence of a phase transition near 15°C. Linear fits to each dataset yield activation energies of 156 ± 6.7 and 79 ± 5.0 kJ/mol for the glassy and fluid phases, respectively. Although the transition from the glassy to the fluid phase occurs at 15°C in the Arrhenius plot, rather than at 12°C as measured by DSC, the broadness of the DSC peak means that complete melting of the DSPE chains does not occur until 15°C. Therefore, the transition temperature of 15°C is consistent with the DSC measurement of the phase transition.

Discussion

DSC data show a sharp, reversible transition in DSPE vesicles at 74°C that corresponds to the lamellar gel-to-fluid (L_β to L_α) phase transition.[24] This is a highly cooperative first-order transition ascribed to the onset of rotational isomerization of the carbon-carbon bonds in the lipid alkyl tails, and is hence described as the chain-melting transition.[18] However, in micelles of DSPE-PEG(2000), the transition at 74°C is absent. This has been previously reported by Kenworthy et al., who did not observe a calorimetric transition in DSPE-PEG(2000) micelles in the range 30°C to 90°C.[19] Here a reversible transition is observed at 12°C that, although broad and therefore not highly cooperative, has a significant transition enthalpy, i.e. latent heat, of 39 ± 4.2 kJ/mol. This transition is not due to a thermotropic event associated with PEG, since neither the DSPE sample with PEG(3400) in solution nor DPPE-PEG(2000) micelles show such a transition. Further, the measured transition enthalpy is close to the reported value of 44 kJ/mol for the DSPE chain-melting transition.[24] Hence, this transition is ascribed to the melting of DSPE lipid chains in the core of the DSPE-PEG(2000) micelle. It would be useful to further characterize the melting transition in the lipid core through the use of spin-label electron spin resonance (ESR) spectroscopy to measure rotational freedom of carbon-carbon bonds in the glassy and fluid-phase cores. Using this technique, Belsito and colleagues have characterized the fluid micellar cores of DPPE-PEG(2000) and DPPE-PEG(5000), but their results are not directly comparable to this work as the phase transition of interest is only observed in DSPE-PEG(2000) micelles with larger lipid tails.[18,25]

Covalent linkage between DSPE and PEG(2000) is required for the disruption of ordered packing in DSPE-PEG(2000) micelles. This is supported by the observation that the presence of PEG(3400) in solution does not shift the melting transition. The broader observed transition is possibly due to interference of PEG with the increased lipid hydration required for the phase transition, either by directly interacting with lipid head groups, or by sequestering water molecules that might otherwise participate in lipid hydration.

WAXS provides insight into the structure of the DSPE-PEG(2000) micelle core both above and below the phase transition. The broad shoulder near $q = 1.5$ Å $^{-1}$ indicates a lack of regular packing of lipid chains at 25°C as well as at 2°C. This indicates that DSPE-PEG(2000) micelles have a fluid core at 25°C and that the chain-melting phase transition does not result in the formation of a gel phase with the crystalline ordering observed in DSPE lamellae. The position of the shoulder shifts to slightly lower q at higher temperature in DSPE-PEG(2000) samples, indicating larger average carbon-carbon spacing, as expected for higher temperature.

DLS measurements on DSPE-PEG(2000) micelles indicate that the phase transition seen in DSC does not cause a dramatic shape transition (i.e. spheres to rods or bilayers), as micelle hydrodynamic diameter and q-dependence of this measurement is consistent with small, spheroidal micelles at all temperatures studied. Little contribution to the change in micelle size is expected from the height of the PEG corona over this small range of absolute temperature. Scaling theory of a polymer brush predicts that brush height is proportional to $\nu^{1/3}$, where ν is a dimensionless excluded volume parameter (i.e. $\nu \sim 1–2\chi$ where χ is the Flory-Huggms interaction parameter)2.[26] The excluded volume parameter is assumed to be proportional to the number of water molecules that move with each PEG monomer, i.e. the extent of PEG hydration, which has been shown experimentally to decrease slightly with increasing temperature.[27] Therefore, some decrease in ν is expected as temperature increases, but because the effect on corona height goes as $\nu^{1/3}$, this contribution should be minimal. Similarly, little contribution is expected from the volume change of the lipid core. While the DSPE lipid tail in the fluid state is expected to occupy 106% of its volume in the solid state, this effect is only expected to increase the characteristic length scale of the micelle core by 2% ($1.06^{1/3} = 1.02$).[9,18] Given that the micelle core only contributes roughly 2–3 nm to the overall hydrodynamic

radius of 11–16 nm, expansion of the micelle core upon melting should only cause a ~0.1 nm increase in micelle diameter, making it undetectable by DLS. Given the weak expected temperature-dependence of the micelle core and corona sizes, the continuous increase in micelle size upon heating is likely due to increasing aggregation number and subsequent effects on the axial ratio of the spheroidal micelle as minor shape changes are required to pack more PEG-lipids into the micelle. While further investigation is necessary to establish the mechanism of the observed increase in micelle size upon heating, DLS data do show that small, spheroidal DSPE-PEG(2000) micelles persist at temperatures below the phase transition.

The DSC, WAXS, and DLS data point to the existence of an equilibrium micellar glassy phase in DSPE-PEG(2000) below the phase transition temperature of 12°C. Here, the term “glassy” is used to refer to an amorphous solid phase in the micelle core while not ruling out some degree of local ordering between lipid chains. Although the lipid chains are ‘frozen’, exhibiting low configurational entropy below the transition temperature, significant chain alignment and long-range ordering are prevented by micelle geometry. Bulky size of the PEG(2000) head group favors formation of a glassy core by preventing crystalline packing of lipid chains. In lipids, with their relatively short acyl chains, gel-phase crystallinity implies alignment of each lipid with its neighbor. This situation is impossible in spheroidal micelles where some lipids are required to stretch more than others in order to fill the volume of the micelle core at constant density. In order to align, lipids must adopt a nearly-flat geometry that will be imposed on the PEG corona as well. A change from spheroidal to flat geometry is unfavorable for the PEG brush as the volume available to alleviate crowding increases with distance from the tethering surface only in curved geometries. Thus, the entropy of a curved brush increases relative to a flat brush at constant tethering density and this entropic penalty in the PEG brush opposes the enthalpic benefit to lipid chains upon crystallization. This phenomenon prevents equilibrium crystalline ordering in condensed-phase DSPE-PEG(2000) micelles.

An alternative explanation to consider is that flat bilayers are the equilibrium structure of DSPE-PEG(2000) below the phase transition, but that the coalescence of micelles and subsequent rearrangement of monomers to create flat structures with larger aggregation numbers is sufficiently slow that equilibrium is not obtained on the time scale of observation. This explanation seems unlikely given the observation that micelle solutions stored at 5°C maintain a constant hydrodynamic diameter over a period greater than 60 days. Kinetic data suggest that even at 5°C, monomer exchange rates are sufficiently fast that micelles should be able to equilibrate over periods of days, rather than months.

It is important to note that the glassy micellar phase bears similarities to the liquid ordered lamellar phase observed in some lipid systems containing cholesterol, in that there is a lack of crystalline order despite the lipid chains being frozen into an all-trans state.[28,29] However, the micellar glassy phase is distinguished by the fact that the lack of crystalline order is enforced by the aggregate geometry, rather than specific molecular interactions mediated by cholesterol. It has also been shown that in multicomponent mixed micelles comprising DPPC and the surfactant $C_{12}E_8$, the chain-melting phase transition of DPPC below 41°C causes de-mixing of DPPC lipids into a quasi-lamellar structure within a disk-like micelle that has $C_{12}E_8$ end-caps.[30] In contrast, the single-component DSPE-PEG(2000) micelles used here are unable to de-mix to create a lamellar structure as the bulky PEG headgroup enforces a spheroidal geometry at all temperatures.

The transition temperature between the fluid and condensed phase is affected by self-assembled geometry as it influences the entropy of lipid chains. Since lipid chains cannot align properly in spheroidal geometries, disordered lipids in the core of a fluid micelle have greater entropy than lipid chains in a liquid-crystalline bilayer. Condensation to a state with low entropy is

more unfavorable for lipids in spheroidal micelles than in bilayers and the phase transition occurs at a lower temperature for the micelles.

As discussed above, difficulty to compress the PEG head group in a flat brush is responsible for formation of a curved micelle. It is easy to show that the preferred micelle core radius decreases with PEG molecular weight, increasing the entropy change of the lipid upon condensation for smaller core radii. Consequently, the DSPE transition temperature is expected to depend on PEG molecular weight as seen by comparing the melting temperature of DSPE-PEG(2000) (12°C) with that for DSPE-PEG(1000) (54°C). Head group size also affects equilibrium geometry in the condensed state. While DSPE-PEG(2000) remains glassy below its transition temperature, DSPE-PEG(1000) is crystalline at 25°C as seen in Figure 3. Crystalline packing produces larger aggregates, presumably bilayer structures, in DSPE-PEG (1000) samples, as evidenced by visible solution turbidity. DSPE-PEG(1000) exists in micellar form only above its 54°C transition temperature while DSPE-PEG(2000) has a sufficiently large head group to form spheroidal micelles at equilibrium above and below its transition temperature. Kenworthy and colleagues observed a similar transition for DSPE-PEG(350) but not DSPE-PEG(750), a result suggesting that DSPE-PEG(1000) should not exhibit the transition observed at 54°C. Despite this discrepancy regarding the size of PEG necessary to disrupt the DSPE melting transition, both sets of data demonstrate the same trend; larger PEG head groups are more disruptive to lipid bilayer structure.

Size of the lipid tail also affects the phase behavior of PEG-lipid micelles. 16-carbon PEG-lipid, DPPE-PEG(2000), does not exhibit a phase transition above 5°C, as evidenced by the straight line in Figure 2 for these micelles. In this case, the enthalpic benefit to the lipid core upon condensation does not outweigh the loss of lipid chain configurational entropy in the condensed phase, so that only fluid micelles exist at temperatures above 5°C. Extrapolation of this result implies that adding more carbons to the lipid tail will raise the transition temperature of PEG-lipid micelles, as is generally seen in self-assembled lipid systems.[15,31]

Activation energy of monomer desorption from the micelle increases in the glassy phase relative to the fluid phase. To help explain this observation, the enthalpy and entropy difference between the micelle-inserted and the transition state were estimated using absolute rate theory.[32] For the glassy state, $\Delta H^{\ddagger} = 154 \pm 6.7$ kJ/mol, $T\Delta S^{\ddagger} = 93 \pm 6.7$ kJ/mol and $\Delta G^{\ddagger} = 93 \pm 9.6$ kJ/mol while for the fluid state, $\Delta H^{\ddagger} = 76 \pm 5.0$ kJ/mol, $T\Delta S^{\ddagger} = -16 \pm 5.0$ kJ/mol, $\Delta G^{\ddagger} = 92 \pm 7.1$ kJ/mol. These values reflect the change in energy to move PEG-lipids from the micelle into the transition state at 15°C.

The enthalpic contribution to the activation barrier, which favors micelle-inserted PEG-lipids, increases by 78 kJ/mol in moving from the fluid phase to the glassy phase. This change is significantly larger than the latent heat of melting, measured to be 39 kJ/mol. It is often assumed that the high-energy transition state, in which a PEG-lipid monomer is bound to a micelle by just a small portion of its lipid tail, is independent of the properties of the environment from which it is exchanging.[17] The data presented here suggest that this is not the case for DSPE-PEG(2000) micelles as the latent heat of melting only explains about half of the total enthalpic contribution to the change in activation energy. It is possible that an additional enthalpic penalty may arise from a change in the transition state between fluid and glassy phases. Whereas the fluid micelle may quickly rearrange its molecular packing to accommodate the void left by a PEG-lipid moving into the transition state, this process may happen much slower in a solid micelle as the lateral diffusion coefficient of lipids is expected to decrease by an order of magnitude upon freezing.[33] If the rate at which the micelle core can rearrange to fill the void left by a transition state PEG-lipid is slower than the rate at which the PEG-lipid can create this void, more water molecules will interact with hydrophobic tails in the void, decreasing hydrogen bonding possibilities for those water molecules. This explanation is reasonable given

that the gap in enthalpy of 39 kJ/mol can be explained by the disruption of only two hydrogen bonds with enthalpy of approximately 20 kJ/mol.[34]

In the fluid phase, entropy ($T\Delta S^{\ddagger}$) favors the micelle-inserted state. This is likely due to the fact that the lipid chain entropy is similar in both the fluid and transition states but that water entropy decreases upon solvation of the lipid tail. Upon freezing, the chain entropy in the micelle decreases dramatically, and the entropic term favors the transition state. The magnitude of this change (77 kJ/mol) is greater than the 39 kJ/mol that would be expected for the entropic contribution to freezing in DSPE or DSPC lipid bilayers.[18] This can be partially explained by the fact that the fluid-phase chain entropy is greater in a curved micelle than a planar bilayer but this effect of curvature has not been quantified. Additionally, there may be entropic contributions from water arising from the previously discussed differences between the transition states of glassy and fluid micelles.

Values for activation energy reported are comparable in magnitude to those found for large, unilamellar DMPC vesicles (LUVs).[17] Activation energy was found to be greater in the gel-phase relative to the fluid phase, but further quantitative comparison is obfuscated by differences in the size of the lipid tail, character of the head group, and self-assembled geometry. In contrast to LUVs, activation energy was observed to decrease for the gel phase relative to the fluid phase in small unilamellar DMPC vesicles (SUVs).[17,35] This was attributed to the fact that defect regions in gel-phase SUVs are more disordered than the fluid liquid-crystalline phase, making them more easily expelled from the bilayer. This explanation requires coexistence of defect regions with defect-free regions; a situation that may not be true for the more highly curved PEG-lipid micelles investigated here. The absence of defect-free regions in glassy DSPE-PEG(2000) micelles is indicated by a lack of any sharp peak in WAXS.

A high activation barrier to monomer desorption from the glassy phase and the associated lower monomer desorption rate is important for micelle stability, as a micelle can only be treated as a nanoparticle over the timescale that it remains aggregated. Slower monomer desorption rates imply that micelles disassemble more slowly upon dilution below their CMC. Consequently, monomers would take longer to nonspecifically associate with serum proteins such as albumin or other hydrophobic structures in their environment. Furthermore, lower monomer desorption and exchange rates mean that mixed micelles will retain their original composition for longer times. For a mixed micelle containing separate targeting and therapeutic components, lower desorption rates are essential for delivery of the entire micelle to its target before being broken up or cleared from circulation.

Conclusion

A phase transition in the core of DSPE-PEG(2000) micelles was identified by DSC but interfacial curvature imparted to the micelle by the size of the PEG head group was found to disrupt ordered lipid packing in both phases. Packing disruption in the lipid core, caused by large PEG head group size, resulted in a decreased transition temperature from the fluid to the condensed phase when compared with DSPE lipids. While the phase transition did not significantly change micelle geometry at equilibrium, it did increase activation energy for monomer desorption from the glassy phase relative to the fluid phase.

Micelle stability imparted by a decreased monomer desorption rate is important for *in vivo* applications in which mixed micelles in the glassy phase can remain intact over longer periods of time than fluid-phase micelles. For practical purposes, the transition in DSPE-PEG(2000) micelles occurs at temperatures below those of physiological interest. However, the sizes of the lipid tail and PEG head group were shown to affect this transition temperature. A sufficiently large PEG head group provides a barrier to regular chain packing and favors highly

curved spheroidal micelles at the expense of lowering the phase transition temperature of the lipid core. On the other hand, increased lipid tail length raises the activation energy for monomer desorption from both fluid and glassy phases as well as the transition temperature between the phases. Thus, further investigation of different PEG-lipid monomers may reveal optimal building blocks for highly stable micellar nanoparticles.

Acknowledgments

This work was supported by National Heart, Lung and Blood Institute grants U01 HL080718 and 5 U54 CA119335-04, and in part by the MRSEC Program of the National Science Foundation under award DMR05-20415. The authors are grateful to Prof. Cyrus Safinya, Dr. Youli Li, Morito Divinagracia, and Nate Bouxsein for assistance with x-ray scattering, and to Dr. Krystyna Brzezinska for help with DSC experiments.

References

1. Torchilin VP. Pharmaceutical Research 2007;24:1–16. [PubMed: 17109211]
2. Lukyanov AN, Torchilin VP. Advanced Drug Delivery Reviews 2004;56:1273–1289. [PubMed: 15109769]
3. Sugin Z, Yuksel N, Baykara T. European Journal of Pharmaceutics and Biopharmaceutics 2006;64:261–268. [PubMed: 16884896]
4. Karmali PP, Kotamraju VR, Kastantin M, Black M, Missirlis D, Tirrell M, Ruoslahti E. Nanomedicine: Nanotechnology, Biology and Medicine 2008;5:73–82.
5. Sawant RR, Sawant RM, Torchilin VP. European Journal of Pharmaceutics and Biopharmaceutics 2008;70:51–57. [PubMed: 18583114]
6. Hayama A, Yamamoto T, Yokoyama M, Kawano K, Hattori Y, Maitani Y. Journal of Nanoscience and Nanotechnology 2008;8:3085–3090. [PubMed: 18681050]
7. Accardo A, Tesauro D, Aloj L, Tarallo L, Arra C, Mangiapia G, Vaccaro M, Pedone C, Paduano L, Morelli G. Chemmedchem 2008;3:594–602. [PubMed: 18167625]
8. Peters D, Kastantin M, Kotamraju VR, Karmali PP, Gujraty K, Tirrell M, Ruoslahti E. Submitted. 2009
9. Arleth L, Ashok B, Onyuksel H, Thiyagarajan P, Jacob J, Hjelm RP. Langmuir 2005;21:3279–3290. [PubMed: 15807565]
10. Maeda H, Wu J, Sawa T, Matsumura Y, Hori K. Journal of Controlled Release 2000;65:271–284. [PubMed: 10699287]
11. Alexis F, Pridgen E, Molnar LK, Farokhzad OC. Molecular Pharmaceutics 2008;5:505–515. [PubMed: 18672949]
12. Rejman J, Oberle V, Zuhorn IS, Hoekstra D. Biochemical Journal 2004;377:159–169. [PubMed: 14505488]
13. Ashok B, Arleth L, Hjelm RP, Rubinstein I, Onyuksel H. Journal of Pharmaceutical Sciences 2004;93:2476–2487. [PubMed: 15349957]
14. Uster PS, Allen TM, Daniel BE, Mendez CJ, Newman MS, Zhu GZ. FEBS Letters 1996;386:243–246. [PubMed: 8647291]
15. Israelachvili, JN. Intermolecular and surface forces. Vol. 2nd ed.. Amsterdam ; Boston: Academic Press; 1992.
16. Brown RE. Biochimica Et Biophysica Acta 1992;1113:375–389. [PubMed: 1450207]
17. Wimley WC, Thompson TE. Biochemistry 1990;29:1296–1303. [PubMed: 2322564]
18. Cevc, G.; Marsh, D. Phospholipid Bilayers: Physical Principles and Models. New York, NY: John Wiley and Sons; 1987.
19. Kenworthy AK, Simon SA, McIntosh TJ. Biophysical Journal 1995;68:1903–1920. [PubMed: 7612833]
20. Knorr R, Trzeciak A, Bannwarth W, Gillessen D. Tetrahedron Letters 1989;30:1927–1930.
21. Fields GB, Noble RL. International Journal of Peptide and Protein Research 1990;35:161–214. [PubMed: 2191922]

22. Narten AH, Levy HA. Journal of Chemical Physics 1971;55:2263–2269.
23. Thomas BN, Safinya CR, Plano RJ, Clark NA. Science 1995;267:1635–1638. [PubMed: 17808182]
24. Seddon JM, Cevc G, Marsh D. Biochemistry 1983;22:1280–1289. [PubMed: 6838853]
25. Montesano G, Bartucci R, Belsito S, Marsh D, Sportelli L. Biophysical Journal 2001;80:1372–1383. [PubMed: 11222298]
26. Halperin A, Tirrell M, Lodge TP. Advances in Polymer Science 1992;100:31–71.
27. Nilsson PG, Lindman B. Journal of Physical Chemistry 1983;87:4756–4761.
28. Mills TT, Tristram-Nagle S, Heberle FA, Morales NF, Zhao J, Wu J, Toombes GES, Nagle JF, Feigenson GW. Biophysical Journal 2008;95:682–690. [PubMed: 18390623]
29. Ipsen JH, Karlstrom G, Mouritsen OG, Wennerstrom H, Zuckermann MJ. Biochimica Et Biophysica Acta 1987;905:162–172. [PubMed: 3676307]
30. Funari SS, Nuscher B, Rapp G, Beyer K. Proceedings of the National Academy of Sciences of the United States of America 2001;98:8938–8943. [PubMed: 11481465]
31. Tanford, C. The hydrophobic effect: formation of micelles and biological membranes. Vol. 2nd ed ed.. New York: Wiley; 1980.
32. Glasstone, S.; Laidler, KJ.; Eyring, H. The theory of rate processes: The kinetics of chemical reactions, viscosity, diffusion and electrochemical phenomena. New York: McGraw-Hill; 1941.
33. D'Angelo G, Wanderlingh U, Nibali VC, Crupi C, Corsaro C, Di Marco G. Philosophical Magazine 2008;88:4033–4046.
34. Suresh SJ, Naik VM. Journal of Chemical Physics 2000;113:9727–9732.
35. McLean LR, Phillips MC. Biochemistry 1984;23:4624–4630. [PubMed: 6498159]

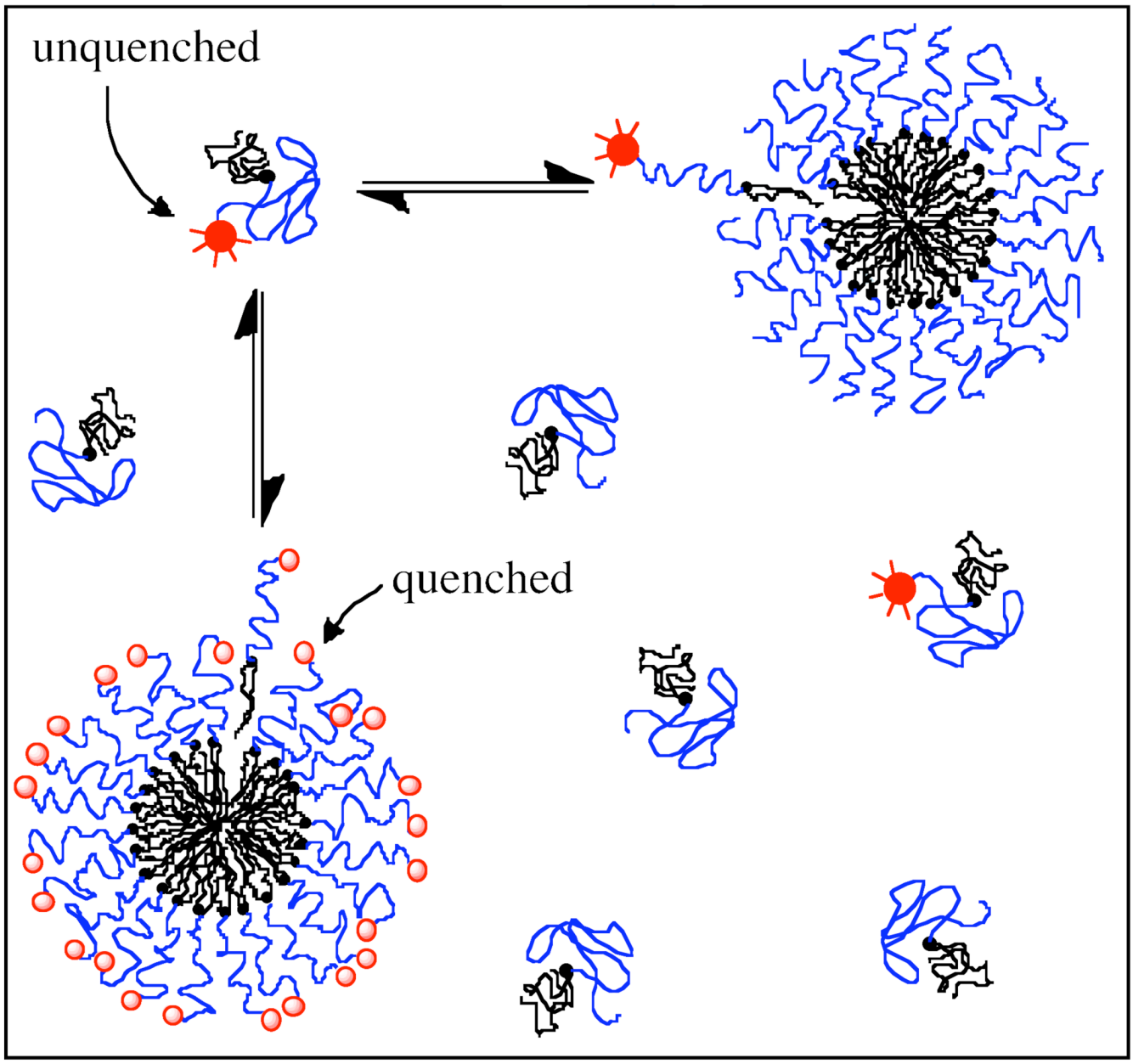

Figure 1.
Monomer desorption rate is measured by fluorescence self-quenching between rhodamine-labeled monomers when micelles with high rhodamine surface density are mixed with unlabeled micelles. Rhodamine fluorescence increases as quenched monomers ( ) leave the densely labeled micelle, becoming unquenched ( ). Unquenched monomers are then free to remain in solution or incorporate into unlabeled micelles.

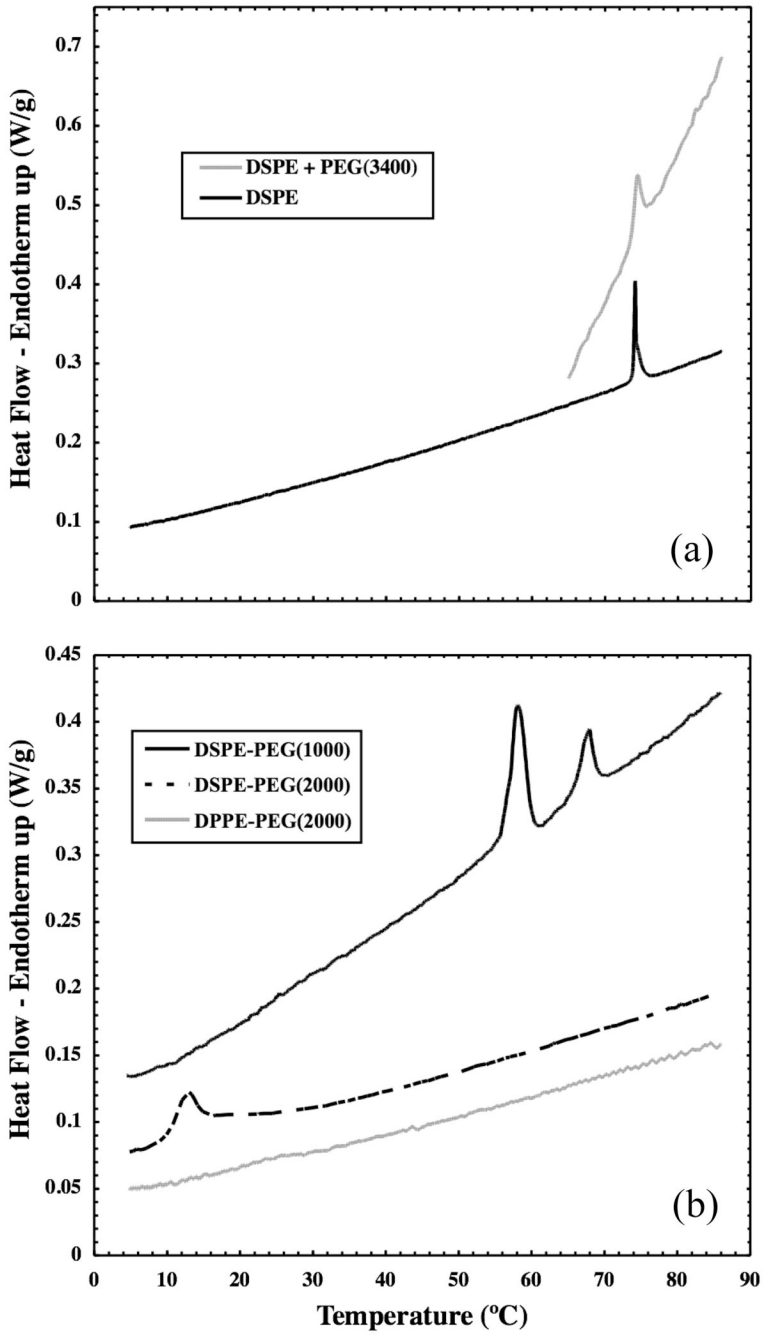

Figure 2.

(a) Differential scanning calorimetry thermograms show a melting transition at 74°C in DSPE vesicles both in the presence and absence of PEG(3400). (b) An endothermic transition upon heating is also seen in DSPE-PEG(2000) micelles at 12.8°C and in DSPE-PEG(1000) micelles at 58.0°C. No transition is seen in DPPE-PEG(2000) micelles. Data have been offset for display purposes.

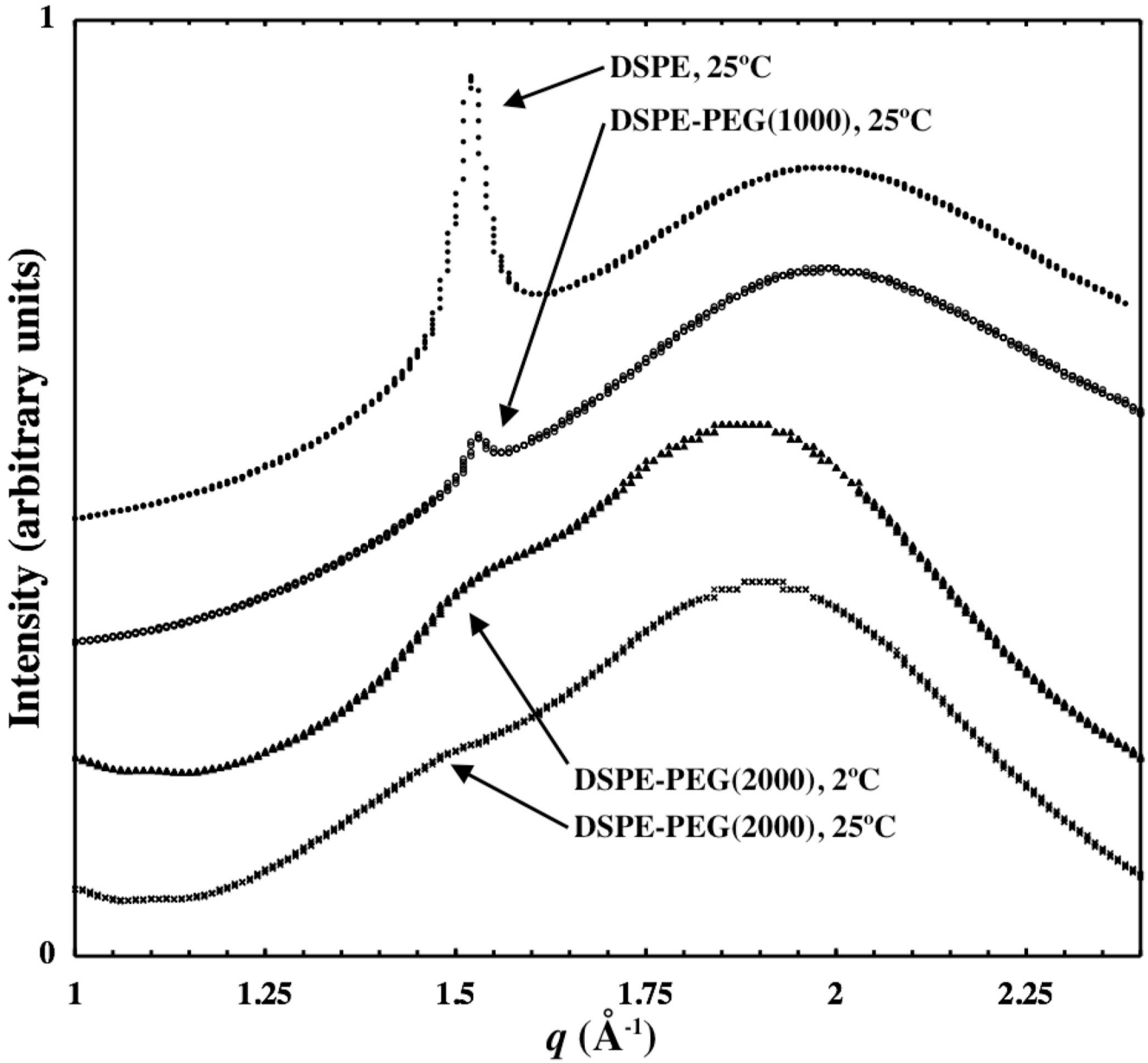

Figure 3.

Wide-angle x-ray scattering data is shown for DSPE, DSPE-PEG(2000), and DSPE-PEG (1000). The broad peak at higher *q* is due to the oxygen-oxygen spacing in water while carbon-carbon spacing in lipid tails gives rise to scattering near 1.5 $Å^{-1}$. Gel-phase DSPE exhibits a sharp peak at 1.53 $Å^{-1}$ while DSPE-PEG(1000) has a similar, albeit smaller, peak (relative to the water peak) at 25°C. DSPE-PEG(2000) micelles exhibit a broad shoulder in this range to indicate that ordered lipid packing is absent at both temperatures. Curves have been offset and arbitrarily scaled for display.

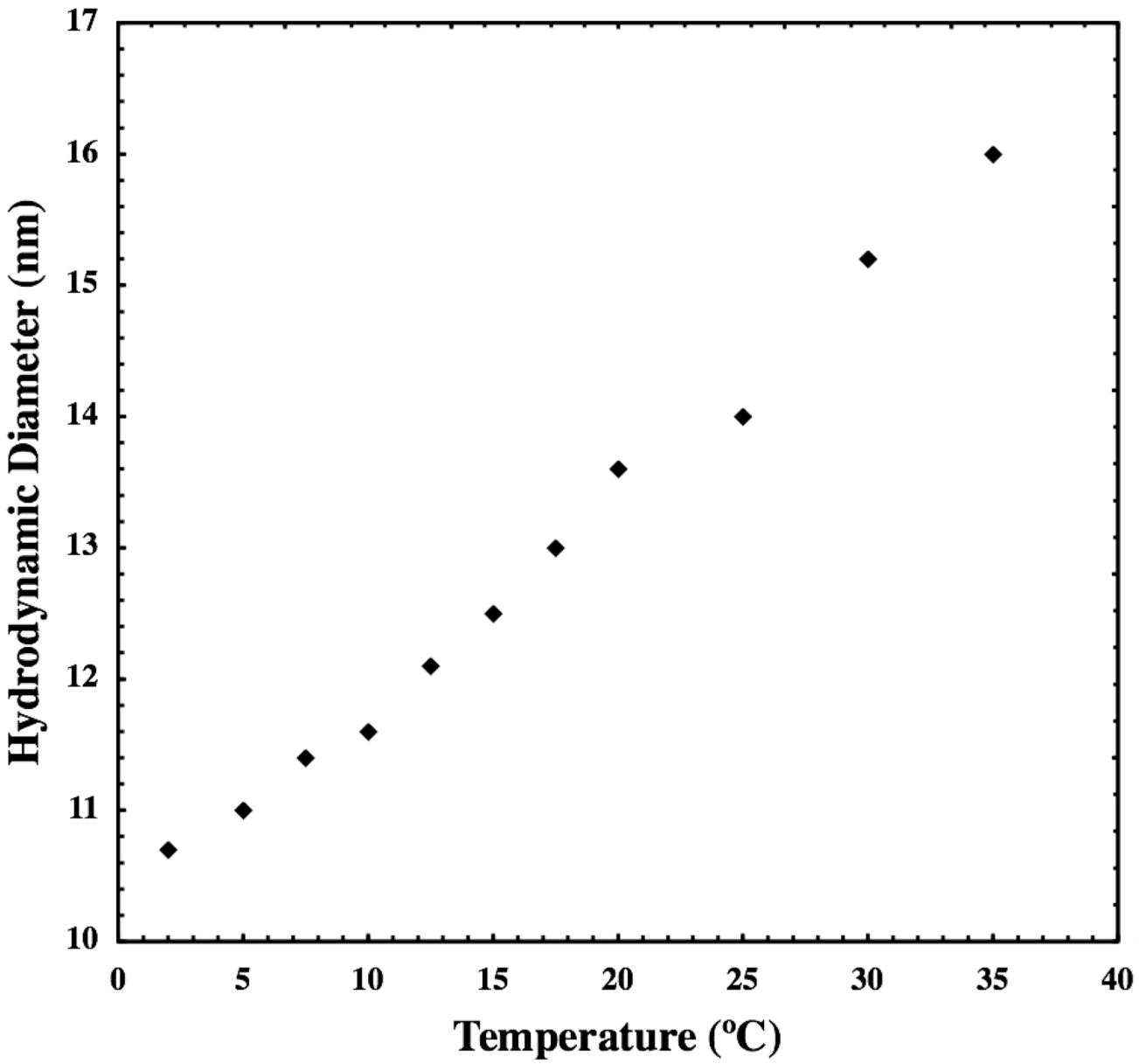

Figure 4.
Hydrodynamic diameter of DSPE-PEG(2000) micelles is shown as a function of temperature. Micelle size remains consistent with small, spheroidal aggregates both above and below their transition temperature.

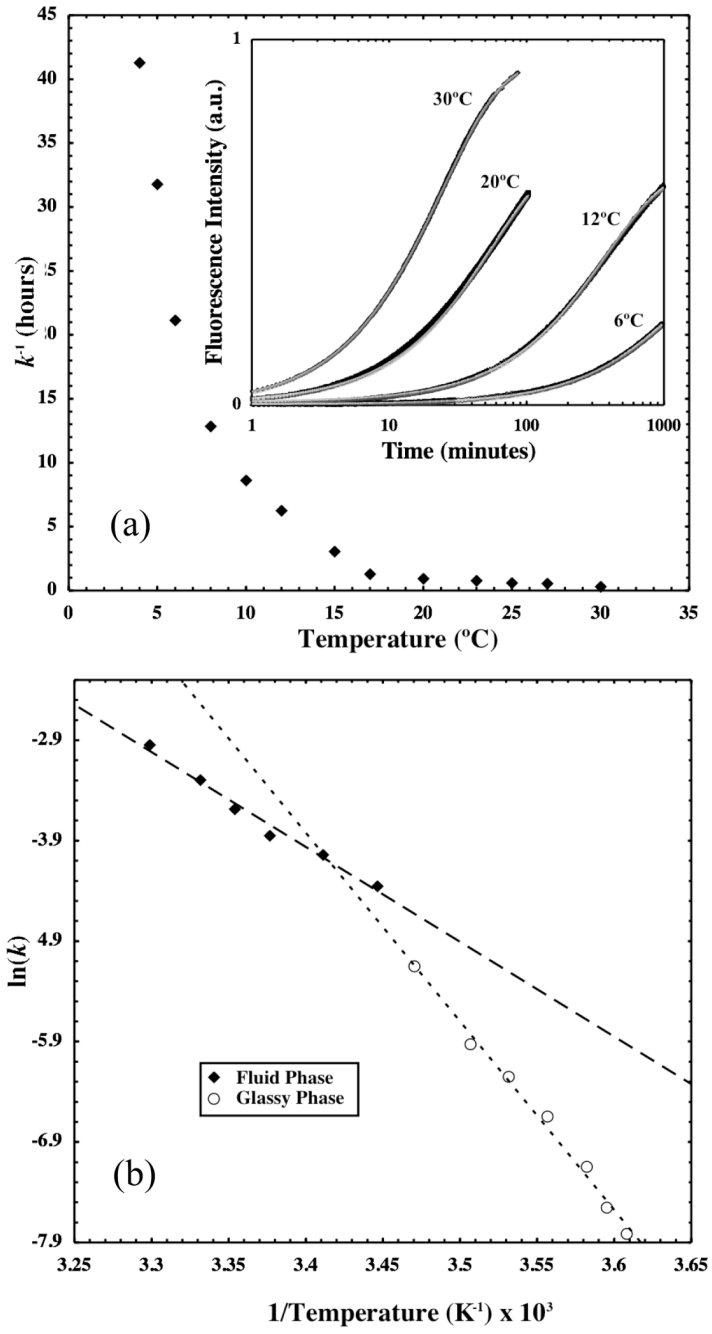

Figure 5.

Desorption rate constants for DSPE-PEG(2000)-RGA are plotted as a function of temperature in (a) while selected raw data along with model fits to the data from equation (2) are shown in the inset. Initial fluorescence intensity has been subtracted from each curve. Kinetic data is presented in an Arrhenius plot in (b). Dashed lines represent linear fits to the data from which the desorption activation energy can be determined.